Title

Nanobodies for accurate recognition of iso-tenuazonic acid and development of sensitive immunoassay for contaminant detection in foods

Authors

Wang, Feng
Yang, Yuan-Yuan
Wan, De-Bin
et al.

Publication Date

2022-06-01

DOI

10.1016/j.foodcont.2022.108835

Peer reviewed

HHS Public Access

Author manuscript

Food Control. Author manuscript; available in PMC 2023 June 01.

Published in final edited form as:

Food Control. 2022 June ; 136: . doi:10.1016/j.foodcont.2022.108835.

Nanobodies for Accurate Recognition of Iso-tenuazonic Acid and Development of Sensitive Immunoassay for Contaminant Detection in Foods

Feng Wang[a], **Yuan-Yuan Yang**[a], **De-Bin Wan**[b], **Jia-Dong Li**[a], **Yi-Fan Liang**[a], **Zhen-Feng Li**[b], **Yu-Dong Shen**[a], **Zhen-Lin Xu**[a], **Jin-Yi Yang**[a], **Hong Wang**[a,c,*], **Jan Gettemans**[d], **Bruce D. Hammock**[b], **Yuan-Ming Sun**[a]

[a]Guangdong Provincial Key Laboratory of Food Quality and Safety, College of Food Science, South China Agricultural University, Guangzhou 510642, P. R. China

[b]Department of Entomology and Nematology and UCD Comprehensive Cancer Center, University of California, Davis, California 95616, United States

[c]Guangdong Laboraotry for Lingnan Mordern Agriculture, Guangzhou 510642, P. R. China

[d]Department of Biomolecular Medicine, Faculty of Medicine and Health Sciences, Ghent University, Ghent B-9000, Belgium

Abstract

The accurate analysis of chemical isomers plays an important role in the study of their different toxic effects and targeted detection of pollutant isomers in foods. The *Alternaria* mycotoxins tenuazonic acid (TeA) and iso-tenuazonic acid (ITeA) are two isomer mycotoxins with the lack of single analysis methods due to the similar structures. Antibody-based immunoassays exhibit high sensitivity and superior application in isomer-specific determination. Previously, various kinds of antibodies for TeA have been prepared in our group. Herein, highly specific nanobodies (Nbs) against ITeA mycotoxin were selected from immune nanobody phage display library, and one of Nbs, namely Nb(B3G3) exhibited excellent affinity, thermal stability as well as organic solvent tolerance. By molecular simulation and docking technology, it was found that stronger

[*]**Corresponding Author**: (H. Wang) Tel: +86 2085283448. Fax: +86 2085280270. gzwhongd@163.com.

Credit Authorship Contribution Statement

Feng Wang: Conceptualization, Methodology, Software, Validation, Formal analysis, Resources, Visualization, Writing-original draft, Writing-review&editing, Project administration. **Yuan-Yuan Yang**: Methodology, Validation, Formal analysis, Investigation, Resources. **De-Bin Wan**: Methodology, Validation, Formal analysis. **Jia-Dong Li**: Methodology, Formal analysis, Visualization. **Yi-Fan Liang**: Methodology, Formal analysis, Investigation. **Zhen-Feng Li**: Methodology, Formal analysis, Investigation. **Yu-Dong Shen**: Resources, Software. **Zhen-Lin Xu**: Methodology, Resources. **Jin-Yi Yang**: Methodology, Resources. **Hong Wang**: Supervision, Project administration, Funding acquisition, Writing-review&editing. **Jan Gettemans**: Resources, Writing-review&editing. **Bruce D. Hammock**: Resources, Funding acquisition, Writing-review&editing. **Yuan-Ming Sun**: Resources, Project administration.

Appendix A. Supplementary data

The supporting information is available free of charge on the publication's website.

Ethical Approval

All procedures involving animals were performed in accordance with the relevant protective and administrative guidelines for laboratory animals of China.

Declaration of interest

The authors declare no competing financial interest.

interaction between Nb(B3G3) and ITeA lead to higher affinity than that for its isomer TeA. Furthermore, a sensitive indirect competitive enzyme-linked immunosorbent assay (icELISA) was established with a limit of detection (LOD) of 0.09 ng/mL for ITeA mycotoxin. The recovery rate of ITeA in spiked samples was analyzed with 84.8%-89.5% for rice, 78.3%-96.3% for flour, and 79.5%-90.7% for bread. A conventional LC-MS/MS method was used to evaluate the accuracy of this proposed icELISA, which showed a satisfactory consistent correlation. Since the convenient strategy for nanobody generation by phage display technology, this study provide new biorecognition elements and sensitive immunoassay for analysis of ITeA in foods.

Graphical Abstract

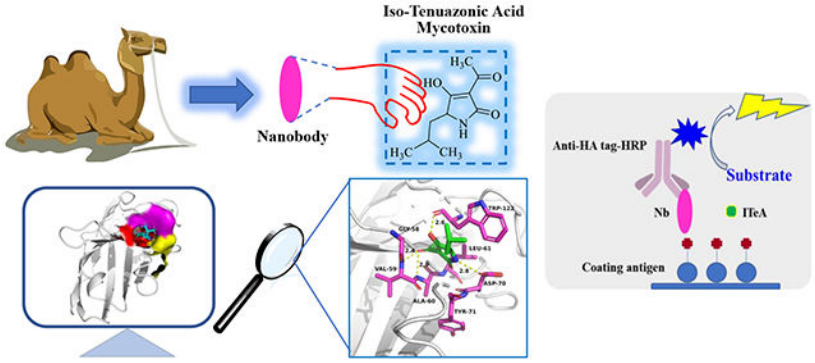

Keywords

Iso-tenuazonic Acid; Mycotoxin Isomer; Nanobody; Accurate Recognition; ELISA

1. Introduction

Different compound isomers can cause completely different toxic effects or other biological effects in animals and humans, which shows that how the isomers could be accurately identified is a very important and meaningful topic (Pan et al., 2018; Kachur et al., 2020). Tenuazonic acid (TeA) and iso-tenuazonic acid (ITeA) are secondary toxic isomer mycotoxins produced by *Alternaria* fungi, only with slight difference of a methyl group position (EFSA, 2011). They could contaminate various kinds of foods with high exposure. Current studies have shown that the two isomers have similar but different chemical properties and toxic effects, but the conventional instrument methods have large difficulty in achieving their accurate identification and analysis (Hickert et al., 2015; Hövelmann et al., 2016; Kumari et al., 2019). Nowadays, antibody-mediated assays present high accuracy, specificity, and sensitivity. Importantly, isomer-specific determination could be performed easily and successfully by immunoassays, such as ofloxacin, styrene oxide and other small molecule compounds (Shen et al., 2009; Mu et al., 2014). The anti-TeA polyclonal antibodies (pAbs), monoclonal antibodies (mAbs) and nanobodies (Nbs) have been prepared with satisfactory specificity in our previous studies (Wang et al., 2018; Liang et al., 2020; Wang et al., 2020). However, in terms of immunodetection of ITeA mycotoxin, only one case was reported with the preparation and application of specific mAb against the complicated derivative of ITeA (Xiao et al., 2018). Thus, development of

new recognition antibodies and immunoassays could greatly expand the accurate analysis of ITeA my cotoxin in foods.

Nanobodies derived from camelid heavy chain antibodies could serve as unique antibodies in immunoassays. In parallel, recent progress in nanobody-based immunoassays are increasingly reported for specific and sensitive detection of toxic pollutants in foods (Bever et al., 2016). They could exhibit superior performance in the enhancement of assay sensitivity, the high stability of thermal treatment, and the tolerance of organic solvent. In terms of the contamination monitoring of mycotoxins in foods, specific nanobodies against aflatoxins, ochratoxins, deoxynivalenol, microcystins, and TeA mycotoxin have been generated and exploited for immunodetection with satisfactory results (Doyle et al., 2008; He et al., 2014; Liu et al., 2014; Pírez-Schirmer et al., 2017; Wang et al., 2020).

Herein, a high-quality nanobody library was generated by the successive immunizations with a *Bactrian* camel. Then, the improved phage display technology was applied to select specific nanobodies against ITeA mycotoxin. The performances of these obtained nanobodies were characterized and molecular simulation was used to illustrate the recognition mechanism of nanobody-ITeA. At last, a sensitive ELISA was developed with indirect competitive strategy, and used to evaluate the recovery of ITeA in spiked samples. The accuracy of the developed assay was validated by liquid chromatography-tandem mass spectrometry (LC-MS/MS).

2. Materials and methods

2.1. Reagents, Materials and Apparatus

ITeA mycotoxin was obtained with a purity of 97.64% (Xiao et al., 2018). Other mycotoxins including TeA, alternariol monomethyl ether (AME), alternariol (AOH), deoxynivalenol (DON), and zearalenone (ZEN) were purchased from Toronto Research Chemicals (Ontario, Canada) and Aladdin Chemical Technology Co., Ltd. (Shanghai, China). The hapten ITeA-CMO was the carboxymethyloxime derivative of ITeA, which was prepared in our laboratory (Figure S1). The immunogen ITeA-CMO-ConA (ITeA-CMO conjugated with carrier protein concanavalin A (ConA)), and the coating antigen ITeA-CMO-OVA (ITeA-CMO conjugated with ovalbumin (OVA)) were used in this study. The secondary antibody goat anti-HA tag labeled with horseradish peroxidase (anti-HA-HRP) was purchased from Roche Molecular Systems, Inc. (Indianapolis, USA). Other molecular biology reagents were purchased from Gbcbio Technologies Inc. (Guangzhou, China), Takara (Dalian, China), QIAGEN (Dusseldorf, Germany) and New England Biolabs (MA, USA). All other chemicals used in this study were from Sigma (St. Louis, USA). The absorbance value was measured on a Multiskan MK3 microplate reader (Thermo Labsystems, USA). LC-MS/MS analysis was conducted on an Agilent SL liquid chromatograph system with 4000 Qtrap mass spectrometer (Agilent Technologies, Santa Clara, USA).

2.2. Construction of Immune Nanobody Library

A male *Bactrian* camel was raised and immunized with ITeA-CMO-ConA as described before (Wang et al., 2020). After five times of immunization, 100 mL fresh blood was

collected in anticoagulant tubes. The one-step PCR was designed for gene amplification of nanobody fragment. The primers of PCR were previous described with slight modification (Li et al., 2012). One-step PCR was conducted with the sense primer P1 (5′-CATGCCATGACTCGCGGCCCAGGCGGCCGTCCTGGCTGCTCTTCTACAAG G-3′), two antisense primers P2-IgG2 (5′-CATGCCATGACTCGCGGCCGGCCTGGCCCGTGCATTCTGGTTCAGGTTTTGGTTG TGG-3′) and P3-IgG3 (5′-CATGCCATGACTCGCGGCCGGCCTGGCCCTTGCATACTTCATTCGTTCC-3′). The recombinant plasmid was electrotransformed into competent cells of *E. coli* ER2738, and the *E. coli* library was infected with helper phage M13K07 for preparation of phage display library. The performance of phage library was assessed for further biopanning.

2.3. Biopanning of Nanobodies against ITeA

The phage-displayed biopanning was designed with four rounds using the coating antigen of ITeA-CMO-OVA. The procedures of panning were described before with slight modification (Wang et al., 2020). The detail information was listed in Table 1. A series of gradient concentration of coating antigen (12.5, 2.5, 0.5, 0.1 μg/mL) were coated in the wells of 96-well microplate. In order to eliminate the nonspecific binding, two kinds of blocking buffer including 1% fish gelatin in PBS buffer and 3% skimmed milk in PBS buffer were prepared for blocking in the four rounds. The specific phages were eluted with the acid buffer of 0.1 mol/L glycine-HCl buffer (pH 2.2) in the first round, and the competitive elution using 1000 ng/mL, 100 ng/mL, and 10 ng/mL of ITeA was used in other rounds. At last, the clones were picked up from agar plates and cultivated for nanobody expression in deep-well plates. The expression supernatants were collected and assessed by indirect competitive enzyme-linked immunosorbent assay (icELISA). The positive clones were sequenced and analyzed for further study.

2.4. Expression, Purification, and Characterization of Nanobodies

The obtained plasmids were transformed to *E. coli* BL21(DE3). Single clone was picked up and cultivated in 2×YT medium at 37 °C for nanobody expression. The bacteria were collected after centrifugation and the cell lysis was conducted by bacterial protein extraction reagent (B-PER). These obtained Nbs were purified with standard Ni-NTA affinity chromatography and identified by SDS-PAGE. The performances of them were characterized by icELISA.

2.5. Thermal Stability and Organic Solvent Tolerance of Nanobodies

The titer of these nanobodies was determined as the optimal concentration by ELISA with 1 μg/mL of coating antigen ITeA-CMO-OVA. To investigate thermal stability of nanobodies, optimal concentrations of them were separately incubated at 22 °C, 37 °C, 45 °C, 50 °C, 60 °C, 70 °C, 80 °C, 90 °C, and 100 °C for 5 min. For the further study of extreme temperature, these nanobodies were separately operated at 70 °C, 80 °C, and 90 °C from 10 min to 120 min. The analysis of organic solvent tolerance was conducted with several levels of methanol (MeOH) and acetonitrile (ACN) in PBS buffer. After the treatment of thermal or organic solvent, the activity of these nanobodies was analyzed by ELISA and compared with

the original activity. It was calculated that relative activity (%) = (the treatment activity/the original activity) × 100.

2.6. Development of Sensitive icELISA for ITeA Detection

The proposed icELISA was conducted with an indirect competitive strategy on the basis of the excellent Nb(B3G3). Firstly, a checkerboard method was used for determination of optimal concentrations of coating antigen ITeA-CMO-OVA and the corresponding Nb(B3G3). More specifically, the wells of microplate were operated to do overnight coating at 37 °C and blocked with 3% skimmed milk for 1 h. After 3-time washing, 50 μL/well of optimal concentrations of Nb(B3G3) and 50 μL/well of gradient concentration of ITeA were added in wells for 40 min-incubation at 37 °C. The wells were supplied with 100 μL/well of anti-HA-HRP (9.1 ng/mL) after washing. The plates were incubated at 37 °C for 40 min, and then conducted with 3-time washing. 100 μL/well of fresh TMB solution was added and incubated at 37 °C for further 10 min to produce enzymatic reaction, then the absorbance values were measured on a Multiskan MK3 microplate reader after the stopping reaction with 10% H_2SO_4.

2.7. Sensitivity and Selectivity of icELISA

The performance of icELISA was determinated from the standard curve with a four-parameter logistic equation using Origin 8.0 (Origin Lab, Northhampton, ME). The half inhibitory concentration (IC_{50}) and the limit of detection (LOD, IC_{10}) were calculated from the standard curves. The IC_{10} value is the ITeA concentration at 10% of maximum value for the specific immunoassay. To analyze the selectivity of icELISA, the cross-reactivity (CR) of Nb(B3G3) with other mycotoxins (TeA, AOH, AME, DON and ZEN) was performed with the calculation formula CR (%) = (IC_{50} of ITeA / IC_{50} of other mycotoxins) × 100.

2.8. Recognition Characteristics of Anti-ITeA Nb(B3G3) by molecular simulation

The 3D model of Nb(B3G3) was built online through the automated protein structure homology-modelling SWISS-MODEL server (https://swissmodel.expasy.org/), and it was evaluated by the online SAVES v6.0 server (https://saves.mbi.ucla.edu/). Then the docking procedures of Nb(B3G3) and ITeA mycotoxin were operated as described before using the LeadIT 2.1.8 software (Fu et al., 2021). The obtained results were created by PyMOL (version 2.4.0a0, open-source).

2.9. Analysis of Spiked Samples by icELISA and LC-MS/MS

Commercial samples (rice, flour, and bread) were purchased from local supermarket in Davis. These samples were analyzed with endogenous content by LC-MS/MS method, and then spiked with different concentrations of ITeA for recovery study. 1 g of crushed sample was extracted with 10 mL of 50 % methanol in distilled water and centrifuged at 20000 rpm for 30 min. The supernatants were used in the analysis by ELISA and LC-MS/MS. Parameters and operation conditions of LC-MS/MS were described before (Wang et al., 2020). The results were fitted with a correlation analysis between ELISA and LC-MS/MS.

3. Results and Discussion

3.1. Isolation and Performance Evaluation of Anti-ITeA Nanobodies

After five times of immunization, the titer of camel serum could reach 1.28×10^5 by ELISA analysis. The one-step PCR was used for amplification of nanobody gene, and the library capacity was 6.88×10^8 cfu/mL. Specific nanobodies against ITeA mycotoxin were selected from the nanobody library using phage display technology. After selection of nanobodies, a total of twenty-five clones were selected and analyzed by non-competitive ELISA. The results in Figure 1A indicated a total of fourteen clones were obtained with significant positive/negative binding values (P/N>2.1). Furthermore, these clones were analyzed by indirect competitive ELISA (Figure 1B), and these positive nanobodies with specificity were selected from the prepared nanobody library. The results of icELISA showed that the three nanobodies named Nb(B3G2), Nb(B3G3), and Nb(O3H2) had higher inhibition rate under 1.0 μg/mL ITeA among these clones. The CDR sequences of them were shown in Figure 2A. They were expressed in *E. coli* BL21(DE3) under the induction of 1.0 mM IPTG and purified by the traditional Ni-NTA resin. After purification, the identification of these three nanobodies by SDS-PAGE was shown in Figure 2B. The yield of Nb(B3G2), Nb(B3G3), and Nb(O3H2) in *E. coli* BL21(DE3) were 0.38, 3.36, and 1.09 mg/L, respectively. The sensitivity of them were characterized by icELISA with similar IC_{50} values (Figure 2C).

3.2. Thermal Stability and Organic Solvent Tolerance of Nanobodies

In this study, the obtained three nanobodies were firstly treated under various temperature for 5 min. The activity of them could maintain ~100% of the original activity at 50 °C, ~80% activity at 80 °C, even ~70% activity at 100 °C for 5 min (Figure 3A). During the treatment of extreme temperature for 10-120 min, these nanobodies were detected with over 50% of antibody activity at 80 °C for 20 min and 100 °C for 10 min (Figure 3B and 3C). Furthermore, these nanobodies were incubated in PBS buffer containing MeOH or ACN. Results showed that they had ~100% of antibody activity in 10% MeOH and 5% ACN in PBS, even possessed ~5% activity in 80% MeOH and 40% ACN (Figure 3D). These findings were consistent with that of other nanobodies (He et al., 2014; Chen et al., 2016; Liu et al., 2017; He et al., 2019). It was indicated that these obtained nanobodies had excellent performance including outstanding thermal stability and organic solvent tolerance, which were attributed to the unique structure of nanobodies (Muyldermans, 2013; Kunz et al., 2017; Kunz et al., 2018).

3.4. Sensitivity and Selectivity of Nb(B3G3)-based icELISA for ITeA Detection

Considering the yield and sensitivity of the obtained nanobodies, the unique Nb(B3G3) was selected for establishment of ELISA with indirect competitive strategy. The standard curve was shown in Figure 4. The IC_{50} value was calculated as 1.3 ng/mL with the LOD value of 0.09 ng/mL, which was 6-fold improvement compared with that of the previous results for ITeA detection (Xiao et al., 2018). The selectivity of icELISA was determined by analysis of cross reactivity of the assay. Other mycotoxins were used for development of standard curves to compare with the original one with ITeA mycotoxin. As shown in Table 2, there was no obvious CR with the four mycotoxins (AME, AOH, DON, and ZEN), which were driven mainly by the obvious difference of their structures (Wang et al., 2018). The CR of

6.6% with TeA showed that there were weak common binding characteristics and strong specific uniqueness in the recognition of ITeA and TeA with anti-ITeA Nb. The generated Nb(B3G3) present excellent sensitivity and specificity, and the developed icELISA was developed for immunodetection of ITeA mycotoxin.

3.5. Recognition Characteristics of Anti-ITeA Nb(B3G3) and ITeA Mycotoxin

To investigate the recognition mechanism of Nb(B3G3) against ITeA mycotoxin, the sequence of Nb(B3G3) was blasted online with SWISS-MODEL workspace and the 3D structure model was built on the template of crystal structure of the camelid nanobody (PDB: 4tvs). The obtained model was evaluated with the VERIFY3D, ERRAT and PROCHECK evaluation. 93.8% of the residues have averaged 3D-1D score over 0.2 in evaluation of VERIFY3D (Figure S2A). The overall quality factor of ERRAT was 85.714 (Figure S2B). The PROCHECK results of Ramachandran plot indicated that 94.5% of Nb(B3G3) residues were located in most favoured regions, and there were no residues located in disallowed regions (Figure S2C). All these results could meet the requirements of this homology model. This 3D model of Nb(B3G3) was used for ligand docking with ITeA to obtain key amino acid residues of specific recognition. The recognition mode of Nb(B3G3) and ITeA was shown in Figure 5A. It was indicated that the ITeA molecule was deeply buried in the pocket formed by specific residues in FR2, FR3 and CDR3 of Nb(B3G3) (Figure 5B). The specific binding between Nb(B3G3) and ITeA was driven by four main hydrogen bonds (Val59, Ala60, Asp70, and Trp122) and some weaker hydrophobic forces (Gly58, Leu61, and Tyr71). The docking score of Nb(B3G3)-ITeA was −14.4229 with four stronger hydrogen bonds (2.4, 2.6, 2.8, and 2.9 Å). Although TeA had similar structure with ITeA, it present big difference in molecular electrostatic potential isosurfaces of them (Wang et al., 2018). The results in Figure 5C showed that the docking score of Nb(B3G3)-TeA was −12.8947 with only three hydrogen bonds (2.5, 2.6, and 2.8 Å). These reasons contributed to the low recognition of anti-ITeA Nb(B3G3) with TeA. The similar results were obtained for the anti-TeA nanobody with lower reactivity with ITeA by molecular simulation (data not shown). Meanwhile, highly accurate nanobody against ITeA could be generated by phage display technology, which was similar to the specific anti-TeA nanobody prepared by the similar method (Wang et al., 2020).

3.6. Analysis of Spiked Commercial Samples by icELISA and LC-MS/MS

In order to evaluate practicality of this assay, commercial samples (rice, flour, and bread) were selected for recovery analysis. Firstly, sample matrix was investigated on the influence of assay. Different dilutions of sample matrix extract were used for development of standard curves to be compared with the original one using PBS buffer. It was indicated that a 10-fold dilution could eliminate the matrix effect for rice and flour samples, and bread samples required a higher 20-fold dilution for removal of matrix interference (Figure 6). The recovery analysis was conducted on spiked rice and flour samples (6, 20, and 40 ng/g), and spiked bread (12, 40, and 80 ng/mL). The recoveries for rice, flour, and bread samples were 84.8%-89.5%, 78.3%-96.3%, and 79.5%-90.7% (Table 3). The content of ITeA in spiked samples was validated by LC-MS/MS method. The linear correlation between the content of ITeA obtained from icELISA and LC-MS/MS analysis were fitted with a correlation

coefficient (R^2) value of 0.97 (Figure 7). Thus, the developed icELISA on the basis of Nb(B3G3) present excellent performance for detection of ITeA mycotoxin in food samples.

4. Conclusions

In this study, specific nanobodies against ITeA mycotoxin were selected from the immune nanobody library with gene amplification by one-step PCR. After performance assessment of them, these Nb(B3G2), Nb(B3G3), and Nb(O3H2) were selected and characterized with excellent thermal stability and organic solvent tolerance. With the sensitivity comparison of these nanobodies, the best one named Nb(B3G3) was used for establishment of sensitive icELISA. The icELISA showed a sensitive LOD value of 0.09 ng/mL for ITeA. It was indicated that there was a satisfactory recovery rate of 78.3%-96.3% for ITeA analysis in spiked samples, and a conventional LC-MS/MS was used to verify the accuracy of the proposed icELISA with good consistent correlations. The recognition mechanism of Nb(B3G3) and ITeA mycotoxin was illustrated by molecular simulation, and the key amino acid residues could form stronger interaction with ITeA that its isomer TeA. Therefore, the generation of nanobodies and the development of sensitive icELISA not only has great potential in accurate detection of ITeA mycotoxin in foods, but also provide new strategy for specific analysis of other chemical isomers.

Supplementary Material

Refer to Web version on PubMed Central for supplementary material.

Funding

This work was supported by National Key R&D Program of China (2019YFE0116600), Natural Science Foundation of China (31972157), Key-Area Research and Development Program of Guangdong Province (2019B020211002), Lingnan Modern Agricultural Science And Technology Guangdong Laboratory Independent Scientific Research Project (NZ2021032), Guangdong Province Universities and Colleges Pearl River Scholar Funded Scheme (2017), Guangdong Provincial Key Laboratory of Food Quality and Safety (2020B1212060059), the NIEHS Superfund Research Program (P42 ES04699) and the NIEHS RIVER Award (R35 ES030443-01). F. W. is an awardee of International Training Program for Outstanding Young Scientists in Universities of Guangdong Province (2018YQGP_BS006).

References

Bever CS, Dong JX, Vasylieva N, Barnych B, Cui YL, Xu ZL, Hammock BD, Gee SJ (2016). VHH antibodies: emerging reagents for the analysis of environmental chemicals. Analytical and Bioanalytical Chemistry, 408(22), 5985–6002. 10.1007/s00216-016-9585-x [PubMed: 27209591]

Chen J, He QH, Xu Y, Fu JH, Li YP, Tu Z, Wang D, Shu M, Qiu YL, Yang HW, Liu YY (2016). Nanobody medicated immunoassay for ultrasensitive detection of cancer biomarker alpha-fetoprotein. Talanta, 147, 523–530. 10.1016/j.talanta.2015.10.027 [PubMed: 26592642]

Doyle PJ, Arbabi-Ghahroudi M, Gaudette N, Furzer G, Savard ME, Gleddie S, McLean MD, Mackenzie CR, Hall JC (2008). Cloning, expression, and characterization of a single-domain antibody fragment with affinity for 15-acetyl-deoxynivalenol. Molecular immunology, 45(14), 3703–3713.10.1016/j.molimm.2008.06.005 [PubMed: 18632156]

EFSA panel on contaminants in the food chain. (2011). Scientific opinion on the risks for animal and public health related to the presence of *Alternaria* toxins in feed and food. EFSA Journal, 9(10), 2407. 10.2903/j.efsa.2011.2407

Fu HJ, Chen ZJ, Wang H, Luo L, Wang Y, Huang RM, Xu ZL, Hammock B (2021). Development of a sensitive non-competitive immunoassay via immunocomplex binding peptide for the determination

of ethyl carbamate in wine samples. Journal of Hazardous Materials, 406, 124288.10.1016/j.jhazmat.2020.124288 [PubMed: 33525128]

He JX, Ma SJ, Wu S, Xu JJ, Tian JS, Li J, Gee SL, Hammock BD, Li QX, Xu T (2019). Construction of immunomagnetic particles with high stability in stringent conditions by site-directed immobilization of multivalent nanobodies onto bacterial magnetic particles for the environmental detection of tetrabromobisphenol-A. Analytical Chemistry, 92(1), 1114–1121.10.1021/acs.analchem.9b04177 [PubMed: 31763820]

He T, Wang YR, Li PW, Zhang Q, Lei JW, Zhang ZW, Ding XX, Zhou HY, Zhang W (2014). Nanobody-based enzyme immunoassay for aflatoxin in agro-products with high tolerance to cosolvent methanol. Analytical Chemistry, 86(17), 8873–8880. 10.1021/ac502390c [PubMed: 25079057]

Hickert S, Krug I, Cramer B, Humpf HU (2015). Detection and quantitative analysis of the non-cytotoxic allo-tenuazonic acid in tomato products by stable isotope dilution HPLC-MS/MS. Journal of Agricultural and Food Chemistry, 63(50), 10879–10884. 10.1021/acs.jafc.5b04812 [PubMed: 26633086]

Hövelmann Y, Hickert S, Cramer B, Humpf HU (2016). Determination of exposure to the *Alternaria* mycotoxin tenuazonic acid and its isomer allo-tenuazonic acid in a German population by stable isotope dilution HPLC-MS3. Journal of Agricultural and Food Chemistry, 64(34), 6641–6647.10.1021/acs.jafc.6b02735 [PubMed: 27452834]

Kachur K, Suntres Z (2020). The antibacterial properties of phenolic isomers, carvacrol and thymol. Critical Reviews in Food Science and Nutrition, 60(18), 3042–3053. 10.1080/10408398.2019.1675585 [PubMed: 31617738]

Kumari A, Tirkey NN (2019). Tenuazonic acid: a potent mycotoxin. Recent Trends in Human and Animal Mycology, Springer, Singapore, 203–211.10.1007/978-981-13-9435-5_8

Kunz P, Flock T, Soler N, Zaiss M, Vincke C, Sterckx Y, Kastelic D, Muyldermans S, Hoheisel JD (2017). Exploiting sequence and stability information for directing nanobody stability engineering. Biochimica et Biophysica Acta (BBA)-General Subjects, 1861(9), 2196–2205.10.1016/j.bbagen.2017.06.014 [PubMed: 28642127]

Kunz P, Zinner K, Mücke N, Bartoschik T, Muyldermans S, Hoheisel JD (2018). The structural basis of nanobody unfolding reversibility and thermoresistance. Scientific Reports, 8(1), 1–10.10.1038/s41598-018-26338-z [PubMed: 29311619]

Li JW, Xia LJ, Su YH, Liu HC, Xia XQ, Lu Q, Yang CJ, Reheman K (2012). Molecular imprint of enzyme active site by camel nanobodies: rapid and efficient approach to produce abzymes with alliinase activity. Journal of Biological Chemistry, 287(17), 13713–13721. 10.1074/jbc.M111.336370 [PubMed: 22374998]

Liang YF, Zhou XW, Wang F, Shen YD, Xiao ZL, Zhang SW, Li YJ, Wang H (2020). Development of a monoclonal antibody-based ELISA for the detection of Alternaria mycotoxin tenuazonic acid in food samples. Food Analytical Methods, 13(8), 1594–1602.10.1007/S12161-020-01780-W

Liu X, Tang ZW, Duan ZH, He ZY, Shu M, Wang XX, Gee SJ, Hammock BD, Xu Y (2017). Nanobody-based enzyme immunoassay for ochratoxin A in cereal with high resistance to matrix interference. Talanta, 164, 154–158. 10.1016/j.talanta.2016.11.039 [PubMed: 28107910]

Liu X, Xu Y, Xiong YH, Tu Z, Li YP, He ZY, Qiu YL, Fu JH, Gee SJ, Hammock BD (2014). VHH phage-based competitive real-time immuno-polymerase chain reaction for ultrasensitive detection of ochratoxin A in cereal. Analytical Chemistry, 86(15), 7471–7477.10.1021/ac501202d [PubMed: 24992514]

Mu HT, Lei HT , Wang BL, Xu ZL, Zhang CJ, Ling L,Tian YX, Hu JS, Sun YM (2014). Molecular modeling application on hapten epitope prediction: an enantioselective immunoassay for ofloxacin optical isomers. Journal of Agricultural And Food Chemistry, 2014, 62(31): 7804–7812.10.1021/jf404449n [PubMed: 25069865]

Muyldermans S. (2013). Nanobodies: natural single-domain antibodies. Annual Review of Biochemistry, 82, 775–797.10.1146/annurev-biochem-063011-092449

Pan XL, Cheng YP, Dong FS, Liu N, Xu J, Liu XG, Wu XH, Zheng YQ (2018). Stereoselective bioactivity, acute toxicity and dissipation in typical paddy soils of the chiral fungicide propiconazole. Journal of Hazardous Materials, 359: 194–202. 10.1016/jjhazmat.2018.07.061 [PubMed: 30036749]

Pírez-Schirmer M, Rossotti M, Badagian N, Leizagoyen C, Brena BM, & Gonzalez-Sapienza G (2017). Comparison of three antihapten VHH selection strategies for the development of highly sensitive immunoassays for microcystins. Analytical Chemistry, 89(12), 6800–6806.10.1021/acs.analchem.7b01221 [PubMed: 28494149]

Shen SJ , Zhang F, Zeng S, Tian Y, Chai XJ, Gee SJ, Hammock BD, Zheng J (2009). Development of enantioselective polyclonal antibodies to detect styrene oxide protein adducts. Analytical Chemistry, 81(7), 2668–2677.10.1021/ac8023262 [PubMed: 19245253]

Wang F, Cai J, Eremin SA, Xiao ZL, Shen YD, Tian YX, Xu ZL, Yang JY, Lei HT, Sun YM, Wang H (2018). Fluorescence polarization immunoassay for *Alternaria* mycotoxin tenuazonic acid detection and molecular modeling studies of antibody recognition. Food Analytical Methods, 11(9), 2455–2462. 10.1007/s12161-018-1236-8

Wang F, Li ZF, Yang YY, Wan DB, Vasylieva N, Zhang YQ, Cai J, Wang H, Shen YD, Xu ZL, Hammock BD (2020). Chemiluminescent enzyme immunoassay and bioluminescent enzyme immunoassay for tenuazonic acid mycotoxin by exploitation of nanobody and nanobody-nanoluciferase fusion. Analytical Chemistry, 92(17), 11935–11942.10.1021/acs.analchem.0c02338 [PubMed: 32702970]

Xiao ZL, Wang YL, Shen YD, Xu ZL, Dong JX, Wang H, Situ C, Wang F, Yang JY, Lei HT, Sun YM (2018). Specific monoclonal antibody-based enzyme immunoassay for sensitive and reliable detection of *Alternaria* mycotoxin iso-tenuazonic acid in food products. Food Analytical Methods, 11(3), 635–645. 10.1007/s12161-017-1033-9

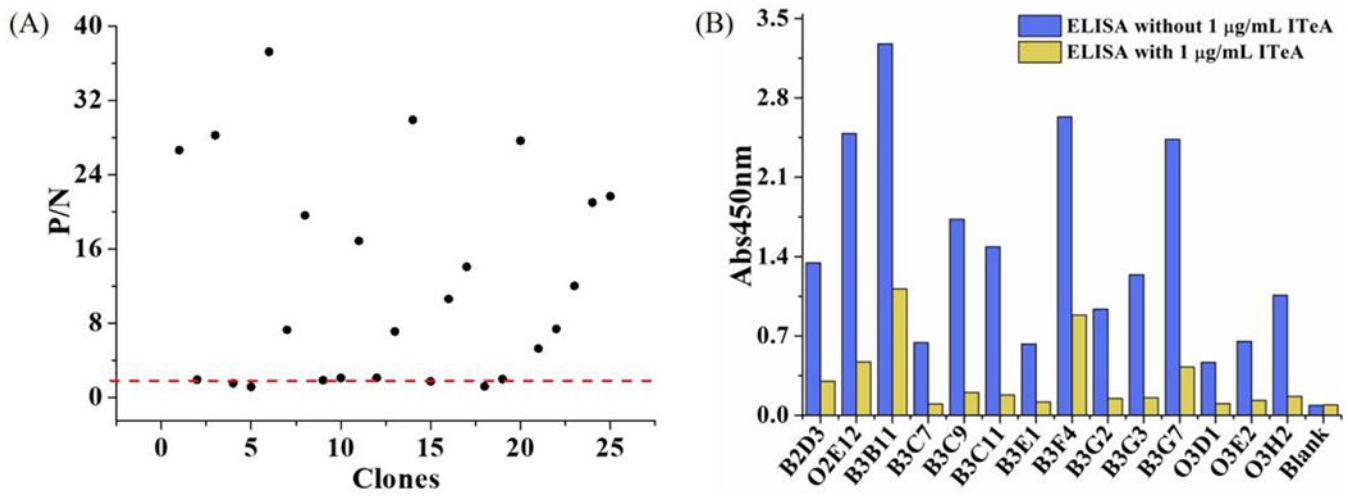

Figure 1.

Identification of expression supernatant of clones by ELISA. (A) Positive/negative values of twenty-five clones analyzed by non-competitive ELISA. (B) the specificity analysis of fourteen clones with P/N>2.1 analyzed by competitive ELISA.

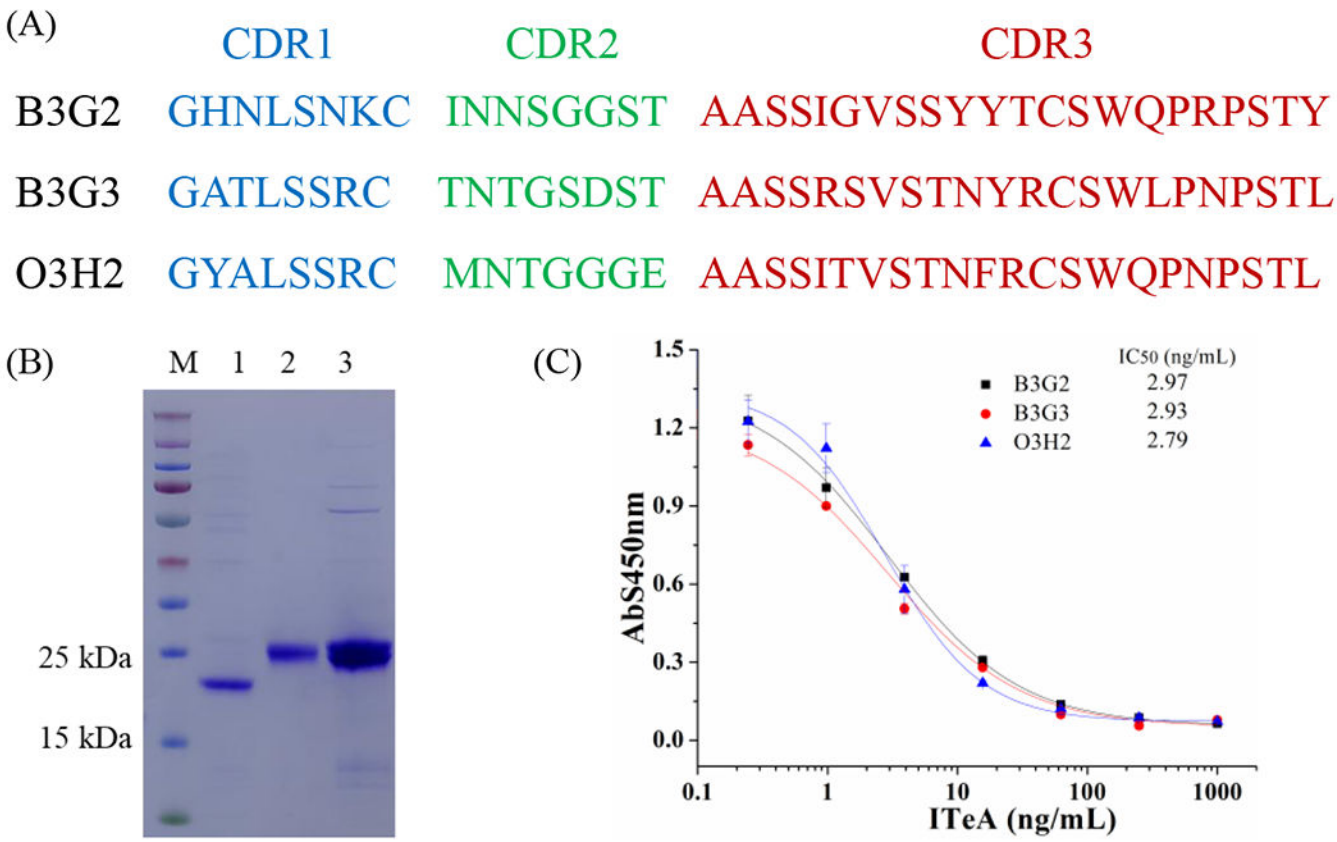

Figure 2.

Performance analysis of these Nb(B3G2), Nb(B3G3), and Nb(O3H2). (A) CDR sequences of anti-ITeA nanobodies, CDR is defined as complementarity determining region of Nb. (B) SDS-PAGE analysis of purified nanobodies. (C) Sensitivities of icELISA on the basis of these obatined nanobodies.

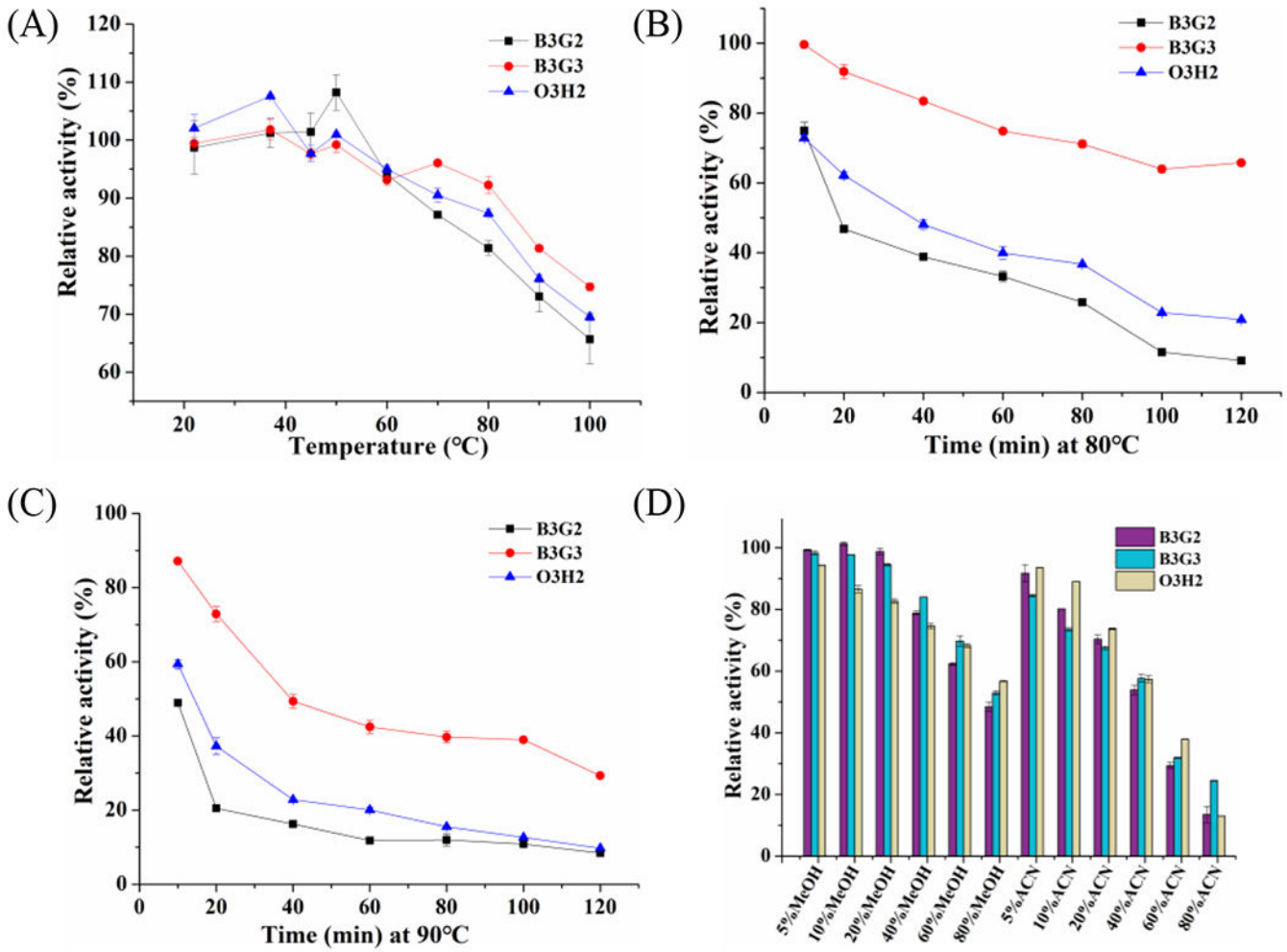

Figure 3.

Assessment of thermal stability and organic solvent tolerance of Nb(B3G2), Nb(B3G3), and Nb(O3H2) by ELISA. (A) Antibody activity analysis of nanobodies incubated separately at different temperatures (22 °C, 37 °C, 45 °C, 50 °C, 60 °C, 70 °C, 80 °C, 90 °C, and 100 °C) for 5 min. (B) Activity analysis of nanobodies incubated at 80 °C for 10-120 min. (C) Activity analysis of nanobodies incubated at 90 °C for 10-120 min. (D) Activity analysis of nanobodies incubated with 5%-80% of MeOH and ACN in PBS buffer.

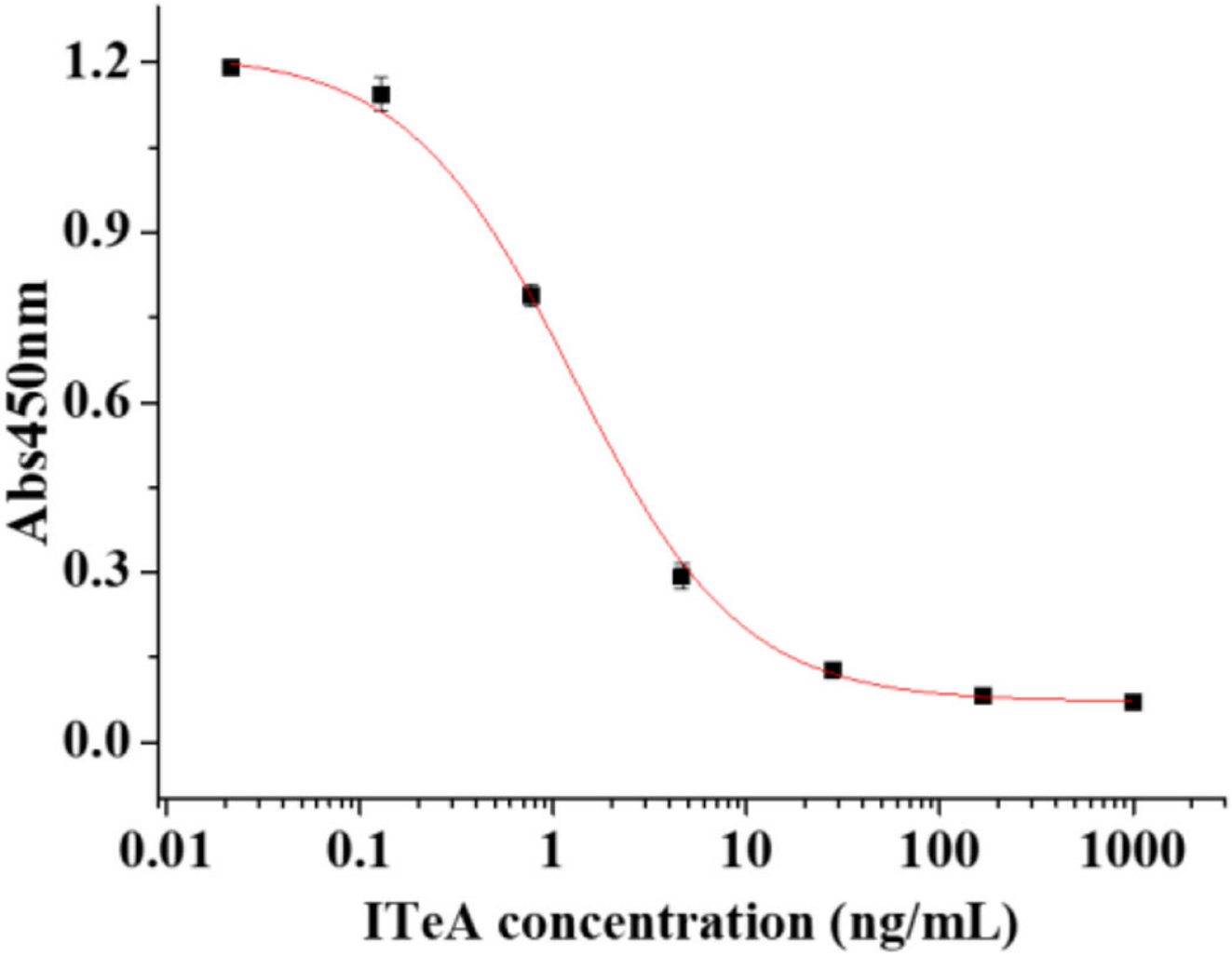

Figure 4.
Standard curve of icELISA on the basis of Nb(B3G3) (n=3).

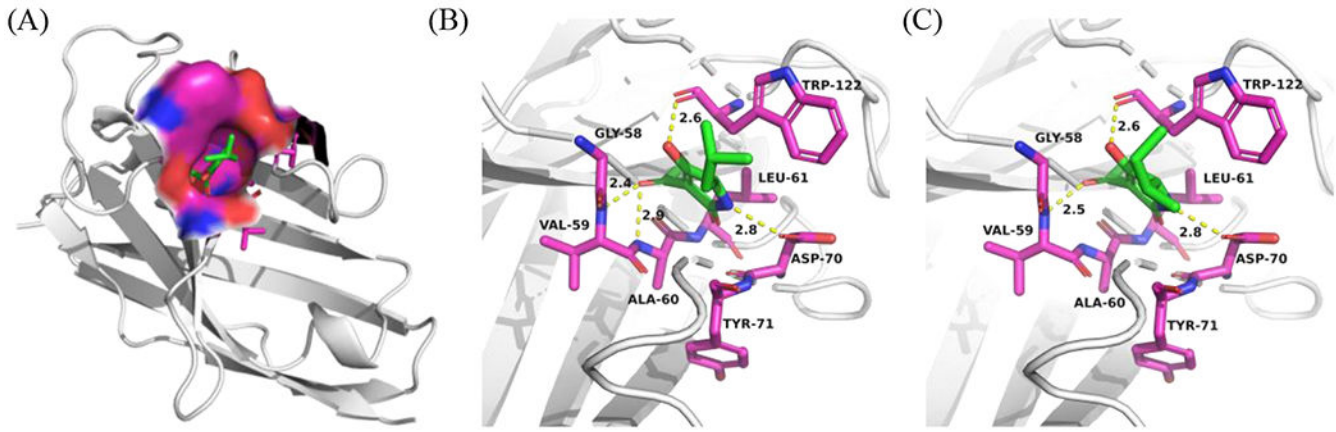

Figure 5.

Recognition characteristics of anti-ITeA Nb(B3G3) and ITeA/TeA mycotoxin. (A) 3D docking map. ITeA was deeply buried in the pocket formed by specific residues in FR2, FR3 and CDR3 of Nb(B3G3). The Gly58, Val59, Ala60, Leu61 in FR2 region were shown in red, Asp70 and Tyr71 in FR3 region were shown in yellow, and Trp122 in CDR3 region was shown in magentas. (B) 2D interaction map of Nb(B3G3) and ITeA. (C) 2D interaction map of Nb(B3G3) and TeA. The key amino acid residues were shown in stick style, and these three main hydrogen bonds (Val59, Asp70, and Trp122) were labeled in yellow dotted line.

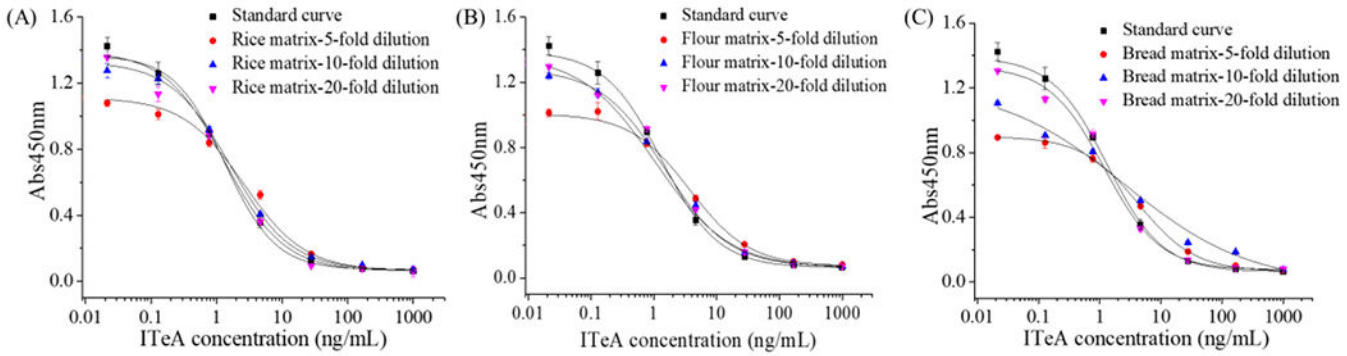

Figure 6.

Studies of sample matrix extracts including rice (A), flour (B), and bread (C) analyzed by icELISA.

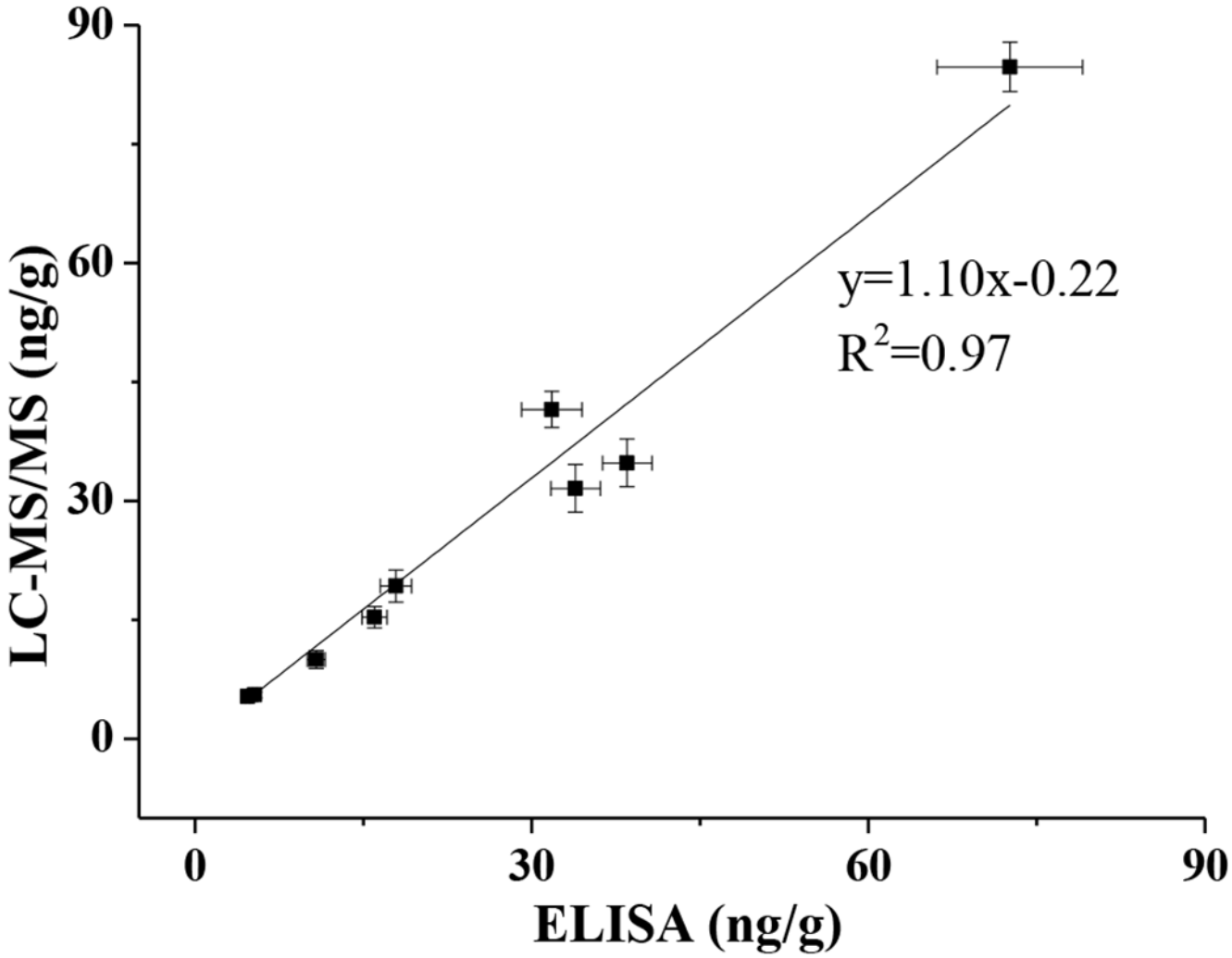

Figure 7.
Correlation analysis between icELISA and LC-MS/MS for ITeA in spiked samples.

Table 1

Panning strategy for anti-ITeA nanobodies by phage display technology

Round	Concentration of coating antigen (μg/mL)	Blocking buffer	Elution method
1	12.5	1% fish gelatin in PBS	acid elution
2	2.5	3% skimmed milk in PBS	competitive elution
3	0.5	1% fish gelatin in PBS	competitive elution
4	0.1	3% skimmed milk in PBS	competitive elution

Table 2

Cross-reactivity determination with other common mycotoxins by icELISA

Analytes	ELSIA	
	IC_{50} (ng/mL)	CR
ITeA	1.3	100%
TeA	19.8	6.6%
AOH	>1000	<1%
AME	>1000	<1%
DON	>1000	<1%
ZEN	>1000	<1%

Table 3

Recovery study of TeA mycotoxin in spiked samples by the developed icELISA and LC-MS/MS

		icELISA			LC-MS/MS		
Samples	**Spiked level (ng/g)**	**Found ± SD (ng/g)**	**Recovery (%)**	**CV (%)**	**Found ± SD (ng/g)**	**Recovery (%)**	**CV (%)**
Rice	6	5.3±0.2	88.3	3.8	5.5±0.4	91.7	7.3
	20	17.9±1.4	89.5	7.8	19.3±2.0	96.5	10.4
	40	33.9±2.2	84.8	6.5	31.6±3.0	79.0	9.5
Flour	6	4.7±0.2	78.3	4.3	5.3±0.4	88.3	7.5
	20	16.0±1.1	80.0	6.9	15.3±1.4	76.5	9.2
	40	38.5±2.2	96.3	5.7	34.8±3.0	87.0	8.6
Bread	12	10.8±0.8	90.0	7.4	10.0±1.1	83.3	11.0
	40	31.8±2.7	79.5	8.5	41.5±2.3	103.8	5.5
	80	72.6±6.5	90.7	9.0	84.7±3.1	105.9	3.7